Received: 22 September 2019 | Accepted: 19 March 2020 | Published online: 20 May 2020

DOI: 10.1002/agj2.20226

Agronomy Journal

ARTICLE

Biofuels

Field and simulation-based assessment of vetivergrass bioenergy feedstock production potential in Texas

Manyowa N. Meki[1] | **James R. Kiniry**[2] | **Abeyou W. Worqlul**[1] | **SuMin Kim**[3] | **Amber S. Williams**[2] | **Javier M. Osorio**[1] | **John Reilley**[4]

[1]Texas AgriLife Research, Blackland Research and Extension Center, 720 East Blackland Road, Temple, TX 76502, USA

[2]Grassland Soil and Water Research Laboratory, USDA Agricultural Research Service, 808 East Blackland Road, Temple, TX 76502, USA

[3]Oak Ridge Institute for Science and Education, 1299 Bethel Valley Road, Oak Ridge, TN 37831, USA

[4]USDA-NRCS, Kika de la Garza Plant Materials Center, 3409 N FM 1355, Kingsville, TX 78363, USA

Correspondence

Manyowa N. Meki, Texas AgriLife Research, Blackland Research and Extension Center, 720 East Blackland Road, Temple, TX 76502, USA.

Email: nmeki@brc.tamus.edu

Funding information

USDA-ARS, Grant/Award Number: 58-6206-1-053

Abstract

Vetivergrass [*Chrysopogon zizanioides* (L.) Roberty] is a multi-purpose crop that has an untapped potential for biofuel production. We conducted a field study at Temple, TX, to determine plant growth characteristics that make vetivergrass an ideal candidate bioenergy feedstock crop. Overall, the high biomass yield (avg. 18.4 ± 0.7 Mg ha^{-1}) can be attributed to the high leaf area index (LAI, avg. 12.7 ± 2.5) and crop growth rates that ranged from 2.7 ± 0.1 to 15.7 ± 0.1 g m^{-2} d^{-1}. Plant tissue N and P concentrations ranged from 0.59–1.66% and 0.06–0.15%, respectively. Surprisingly, the radiation use efficiency (RUE, avg. 2.2 ± 0.1 g MJ^{-1}) was not high relative to other highly productive grasses. Biomass yield was highly correlated to plant height (avg. 2.1 ± 0.1 m) and LAI (Pearson, r = 0.96 and 0.77, respectively). Data from the field experiment provided plant coefficients that were used to develop an Agricultural Land Management Alternatives with Numerical Assessment Criteria (ALMANAC) vetivergrass model to assess dryland and irrigated interannual and spatial biomass yields across Texas. ALMANAC simulated dryland and irrigated yields ranged from 0.8–39.3 (avg. 17.2) Mg ha^{-1} and 9.1–47.0 (avg. 25.4) Mg ha^{-1}, respectively. There was huge spatial variation in dryland and irrigated yields, with CV values of 20 and 15%, respectively. Similarly, dryland and irrigated inter-annual yields respectively had CV values of 25 and 17%. State-wide simulation model assessments complement field studies, and furthermore allow bioenergy companies and investors to better estimate biofuel feedstock potential for new crops such as vetivergrass.

1 | INTRODUCTION

Vetivergrass [*Vetiveria zizanioides* (L.) Nash] now reclassified as [*Chrysopogon zizanioides* (L.) Roberty] (Veldkamp, 1999) is a densely tufted perennial C_4 grass originally domesticated in southern India. The grass is adapted to the tropics and subtropics and can grow on a wide range of conditions: from sands to clays; pH range from 4.0 to 7.5; can tolerate drought, flooding, salinity and a range of heavy metals in the soil (USDA NRCS, 2019a). According to Pinners (2014), vetivergrass thrives in difficult conditions where only a few other plants or grasses will grow. In the US the grass is adapted to the USDA Plant Hardiness Zones 7 to 11 and has done well in Florida, Louisiana, south Texas and Hawaii (USDA NRCS, 2019a).

Abbreviations: ACZs, agroclimatic zones; ALMANAC, Agricultural Land Management Alternatives with Numerical Assessment Criteria; FIPAR, fraction of intercepted photosynthetically active radiation; LAI, leaf area index; PAR, photosynthetically active radiation; RUE, radiation use efficiency.

Vetivergrass is widely promoted by the World Bank for soil and water conservation, beginning in India in the mid-1980s (The World Bank, 1995). The grass can grow up to 2 m in height and has a massive fine root system that can reach depths down to 2 to 6 m in the first year of establishment (Greenfield, 1990; Vieretz, Truong, Gardner, & Smeal, 2003). The deep root system makes the grass tolerant to drought. The tillers are strong and stiff, leaves are narrow and erect, and there is very little lodging. Because of its wide adaptability, the grass is utilized in many ways: *erosion control* – planted as a hedge, it reduces runoff and sediment loss; *stabilization* – rivers, waterways and roads; *phytoremediation and bioremediation* – enhances the degradation of such heavy metals like Al, Cd, Cr, and Cu; *wastewater treatment* - can withstand high levels of N and P in wastewater treatment plants; *perfumery* – vetiver roots contain an essential oil used in many modern perfume creations (Truong & Hengchaovanich, 1997; USDA NRCS, 2019a).

Besides the proven multiple benefits of vetivergrass, the grass is well placed as a potential high biomass energy feedstock due to its high aboveground biomass and a massive deep rooting system which offers huge potential for carbon (C) capture and storage (Figure 1). The grass is propagated vegetatively, and once established needs only moderate inputs for biomass production (Grimshaw, 2004). The grass has the ability to re-grow quickly after harvest and is resistant to most pests and diseases. Furthermore, the grass has a long lifespan and can live up to 50 years without requiring revegetation (National Resource Council, 1993). Because of its wide adaptability, vetivergrass can be grown on marginal lands that do not compete with croplands for food production. In northwest India and Pakistan, vetivergrass has been used to rehabilitate saline areas caused by bad irrigation techniques and drainage practices (Grimshaw, 2004). Dry biomass yields of 70–80 Mg ha^{-1} have been reported (Boucard, 2005; Pinners, 2014). While vetivergrass can be grown as a long-term perennial, it can be easily controlled by glyphosate herbicide or by digging up the crown (USDA NRCS, 2019a). If used as feedstock to generate electricity, vetivergrass has an energy value of 16.3 GJ t^{-1} compared to that of sugarcane bagasse of 9.3 GJ t^{-1} (Pinners, 2014).

While the reported data on vetivergrass dry biomass yields and several rooting depth observations support vetiver's huge potential for C footprint reduction, there is little available information to allow for a more precise accounting of vetivergrass' C sequestration, capture and storage, under different soils, climate, and even different vetiver ecotypes. Available soil C capture and storage estimates range from 12.5–16.4 Mg C ha^{-1} yr^{-1} (Lavania & Lavania, 2009; Singh et al., 2011; Taranet et al., 2011). According to Pinners (2014), for vetivergrass' bioenergy feedstock full potential to be realized, there is need for application of better research technologies and methodologies similar to those being applied to cellulosic ethanol feedstocks like *Miscanthus* and switchgrass (*Panicum virgatum* L.) in the USA and other countries.

Core Ideas

- Vetivergrass bioenergy feedstock potential was assessed using field investigations.
- High biomass is a result of a high leaf area index and high growth rate.
- Field-derived plant parameters were used to develop an ALMANAC vetivergrass model.
- The ALMANAC vetivergrass model was applied to assess interannual and spatial biomass yields across Texas.
- Statewide biomass yield assessments estimate vetivergrass biofuel feedstock potential.

A major reason for the lack of vetivergrass adoption and utilization in the USA is concern about vetivergrass' potential invasiveness. Most cultivars are however naturally sterile and do not set seed (Quinn, Gordon, & Glaser, 2015). The most widely grown cultivar in the USA 'Sunshine' was ranked very low (−8) for the potential to become invasive (USDA NRCS, 2019a). The cultivar has been grown at Sunshine, Louisiana, USA for over 100 years without showing signs of invasiveness. In Hawaii, many farmers grow crops over a range of elevations (from sea level to ∼2,200 m asl) and use 'Sunshine' vetivergrass for erosion control (USDA NRCS, 2019a). Numerous studies in Australia and elsewhere throughout southeast Asia have also showed that most vetivergrass genotypes are sterile, and do not set seed (Truong, 2002).

While the bioenergy industry often cites the uncertainty of dependable feedstock supplies as a major investment risk, potential feedstock growers question the agroclimatic adaptation, production know-how, and sustainability of new feedstock crops, such as vetivergrass. In Texas, agroclimatic regions are generally characterized by an east to west rainfall gradient and a north to south temperature gradient, both of which lead to spatial and temporal variations in productivity (Figure 2). These gradients are confounded by differences in soil type, topography, and management, which amplify variability in agricultural productivity across regions.

The first part of this study focuses on determining and evaluating plant growth characteristics for evaluating vetivergrass as a bioenergy feedstock crop, based on field experiments conducted at Temple, TX, from 2012 to 2014. Field evaluations involved measuring plant parameters that included plant height, leaf area index (LAI), fraction of intercepted photosynthetically active radiation (FIPAR), the light extinction coefficient (k), radiation-use efficiency (RUE), dry biomass accumulation, plant tissue nitrogen (N) and phosphorus (P) concentrations. In the second part, we used data from the

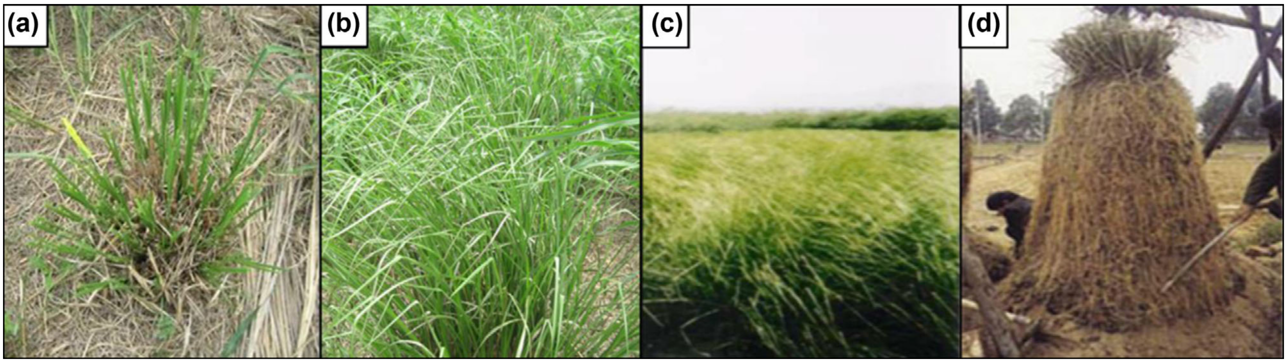

FIGURE 1 Rainfed vetivergrass (cultivar 'Sunshine') at Temple, TX. (a) Green-up stage, (b) 60 days after green-up (DAG), (c) 120 DAG, and (d) vetivergrass root biomass potential; vetiver roots harvested for extracting an essential oil used in perfume creations; photo courtesy of The Vetiver Network International (https://www.vetiver.org/)

field experiment to derive plant parameters for simulating vetivergrass bioenergy feedstock production potential across Texas with an Agricultural Land Management Alternatives with Numerical Assessment Criteria (ALMANAC) model (Kiniry, Williams, Gassman, & Debaeke, 1992).

2 | MATERIALS AND METHODS

2.1 | Study site, plant material, and cultural practices

A rainfed biomass production field trial of vetivergrass cultivar 'Sunshine' was vegetatively established at the USDA ARS, Grassland, Soil and Water Research Laboratory, Temple, TX (31.09° N, 97.36° W; elevation 219 m asl) during the first week of April 2012. The site was previously under the Texas Blackland mixed grass prairie. The soil type is a vertisol, Houston black clay (fine, smectitic, thermic Udic Haplusterts) (Soil Survey Staff, 2011). The Houston Black series consists of very deep, moderately well drained, very slowly permeable soils. A few selected soil properties of the Houston Black clay are presented in Table 1. Weather data for the trial site were from a USDA ARS on-site weather station.

Roundup [*N*-(phosphonomethyl) glycine, $C_3H_8NO_5P$] herbicide was applied at a rate of 3.5 L ha^{-1} a month prior to plowing and disking. The field was fertilized in 2012 with 120 kg N ha^{-1} and 30 kg P ha^{-1} to facilitate better establishment. Planting materials (clumps) were obtained from the USDA NRCS Plant Materials Center at Kingsville, TX. The clumps were split into three to five slips which were then planted during the first week of April at inter- and intra-row spacings of 1 m by 1 m. The total field area for the study was 50 m by 20 m. Two outer planting stations were used as borders on all four sides of the field, leaving a total of 736 stations for sampling. A completely randomized repeated measures design with three replicates was used for biomass samplings and field measurements.

No biomass harvests or measurements were taken in 2012 to allow the vetivergrass to fully establish. The grass was mowed in mid-September (when plants had started to senesce) to 15 cm height and allowed to grow back (ratoon) the following 2013 spring season (Figure 1a). No fertilizer was applied in years 2013 and 2014. Fifty-percent 'green-up' (i.e., appearance of the ratoon green leaves) occurred in the first week of April. For analytical purposes, the first day of April was taken as the day of 50% green-up. In both years, the few weeds present were pulled out by hand.

2.2 | Plant growth measurements

In 2013 and 2014, the first biomass harvest and field measurements were taken 52 days after spring green-up (Figure 1a). Plant height was measured before each biomass harvest, from the ground to the tip of the longest leaf. Biomass samples were collected from randomly chosen representative clump areas of 0.5 m by 0.5 m, avoiding previously sampled clump areas or plot edges. The sampling area was smaller than the 1 m by 1 m planting area to ensure measurements were targeted at the plant canopy and not open spaces. Three samples from a total of three reps were collected on each harvest date. A total of seven biomass harvests were made for each year. Measurements and biomass harvests were taken biweekly, except when not possible due to adverse weather conditions. In the laboratory, biomass samples were weighed, and the leaf area determined using a LiCor LI- 3100 leaf area meter (LiCor Inc., Lincoln, NE). The leaf area was used to calculate leaf area index (LAI). Dry biomass was measured after drying the harvested biomass samples in a forced-air drying oven at 70°C to constant weight. Oven-dried samples were analyzed for total tissue N and P concentrations at early, mid- and late growth stages by the Kjehdal Digest and ICP

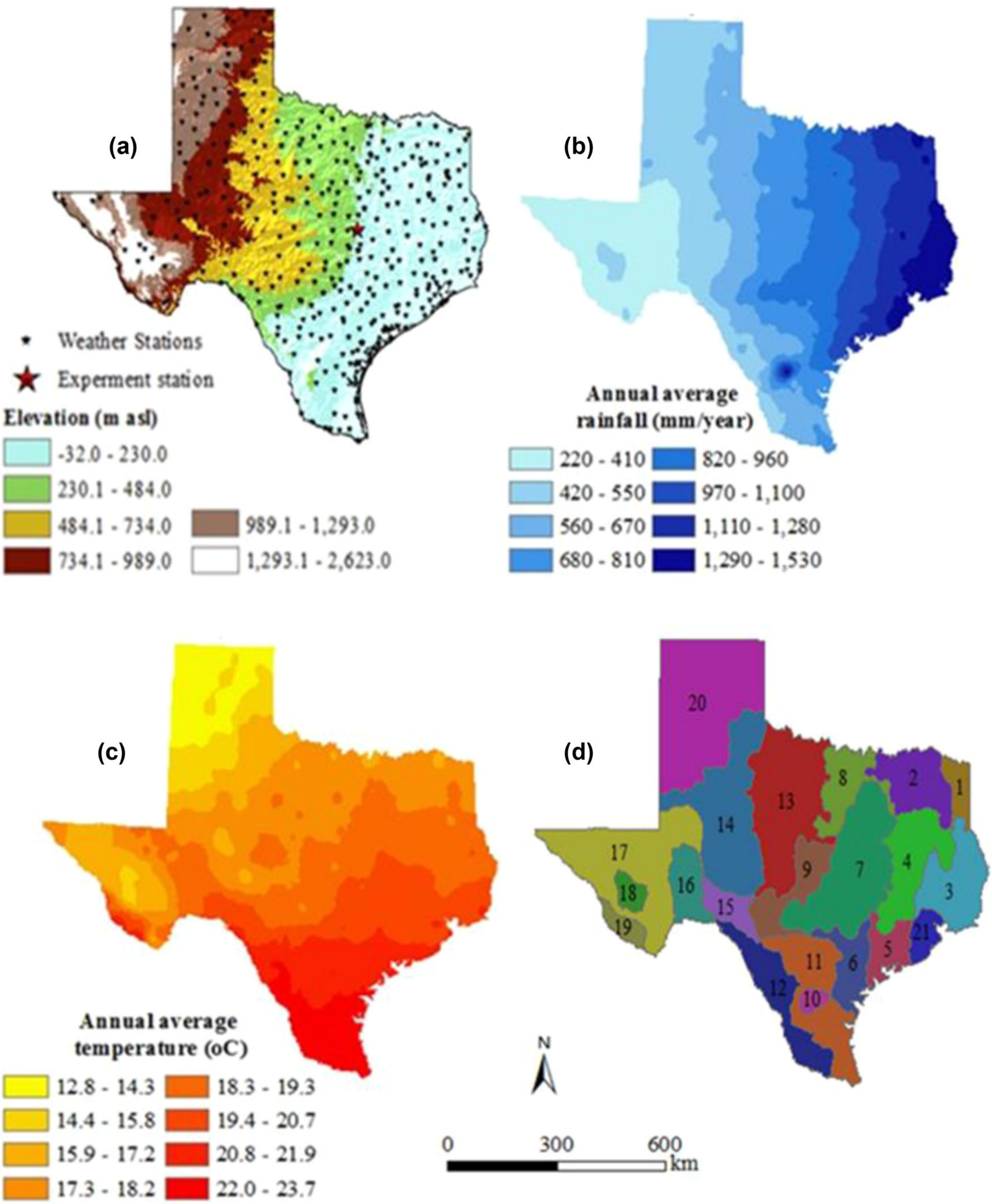

FIGURE 2 (a) Map showing the Temple, TX study site and location of the 455 ALMANAC in-built weather stations used in delineating the agroclimatic zones (ACZs), (b) east to west rainfall gradient, (c) north to south temperature gradient, and (d) the 21 delineated ACZs based on 30-yr (1980–2010) annual average rainfall and temperature. The ACZs along with other complementary information can be found in Tables 4 and 5. Caution: ACZs apply to this study only and should not be used for any other purpose!

methods, respectively, at the Soil, Water, and Forage Testing Laboratory at Texas A&M University, College Station, TX.

The intercepted photosynthetically active radiation (IPAR) was measured with a 0.8 m AccuPAR LP-80 Ceptometer (Decagon, Pullman, WA) as described in Kiniry, Tischler, and Van Esbroeck (1999). The radiation use efficiency (RUE) of the vetivergrass was calculated as the slope of the regression equations for dry biomass as a function of accumulated IPAR. Daily incident PAR was calculated as 45% of the incident total solar radiation (Meek, Hatfield, Howell, Idso, & Reginato, 1984; Monteith, 1965). The light extinction coefficient (k) values for each biomass harvest were calculated using the Beer-Lambert equation as originally described by Monsi and Saeki (1953):

TABLE 1 Selected soil variables for the Houston black clay (0–1%) at the Temple, TX experimental site

Soil variable	Houston black clay (0–1%)		
Soil layer number	1	2	3
Depth (m)	0.01–0.15	0.15–1.12	1.12–2.03
Porosity (mm)	0.53	0.5	0.44
Field capacity (mm)	0.45	0.42	0.4
Wilting point (mm)	0.32	0.3	0.28
Soil water (mm)	0.43	0.4	0.38
Saturated conductivity (mm h^{-1})	1.46	1.46	1.46
Bulk density, oven dry soil (t m^{-3})	1.22	1.31	1.43
Sand (%)	17	17	17
Silt (%)	28	28	28
Clay (%)	55	55	55
Rock (%)	2	2	4
pH	7.9	7.9	7.9
CEC (cmol kg^{-1})	45	45	32.5
Soil organic carbon (%)	1.32	0.23	0.03

Data source: USDA NRCS SSURGO database: https://www.nrcs.usda.gov/wps/portal/nrcs/detail/soils/survey/?cid = nrcs142p2_053627 (accessed 12 Oct. 2019).

$$k = [Ln(1.0 - \text{FIPAR})]/\text{LAI}$$

where FIPAR is the fraction of IPAR.

2.3 | Modeling vetivergrass bioenergy feedstock production potential

2.3.1 | ALMANAC model: release 1203

The model operates on a daily time step and was designed to simulate the major physical and biological processes of agricultural systems, including weather, hydrology, farming operations, crop growth, development and yield, the movement of water, soil carbon storage, nutrients, and sediment at field level. We applied ALMANAC to assess vetivergrass' bioenergy feedstock production potential under rainfed and irrigated conditions across Texas. We chose ALMANAC because of its versatile database infrastructure that combines soils, climate, plant growth characteristics, with management practices that can easily be adapted for various cropping systems. Schema on how the various databases are connected to the ALMANAC engine and how the model operates are provided in the supplemental materials.

2.3.2 | Model set-up

To adequately capture the impacts of the Texas east to west rainfall and north to south temperature gradients on feedstock productivity, we conducted ALMANAC model simulations on 21 agroclimatic zones (ACZs) across Texas. The ACZs were categorized by delineating areas with similar annual average climate characteristics, namely rainfall and temperature based on 455 Texan weather stations from 1980 to 2010: 31-yr timescale (Figure 2). Agroclimatic zonation has previously been used to study the potential impacts of climate change on ecosystems and the environment (Metzger, Bunce, Leemans, & Viner, 2008), and to identify potential new production areas for bioenergy crops (EEA, 2007). For each ACZ, the potential land for vetivergrass production was identified from the USGS National Geospatial Data Asset (NGDA) National Land Use Cover Database (NLCD), and consisted mainly of grassland, pasture, and cultivated cropland. While not all this area will be used for feedstock production, it however provides an upper bound estimate of the potential bioenergy feedstock production from vetivergrass. The dominant soil type within each ACZ was identified from the Digital General Soil Map of the United States (STATSGO2, USDA NRCS, 2019b). Each simulated ACZ represents a known acreage that can be scaled-up to allow state level feedstock production estimates.

2.3.3 | Model parameterization and application

We developed and parameterized an ALMANAC vetivergrass model using data and information from the field experiment conducted at Temple. The leaf area development curve (LADC) parameters: the first and second point on optimal LAI curve (DLAP1 and DLAP2), fraction of season when LAI starts to decline (DLAI), and leaf area decline rate (RLAD) were adjusted by iteratively running the ALMANAC model, comparing the simulated and measured maximum

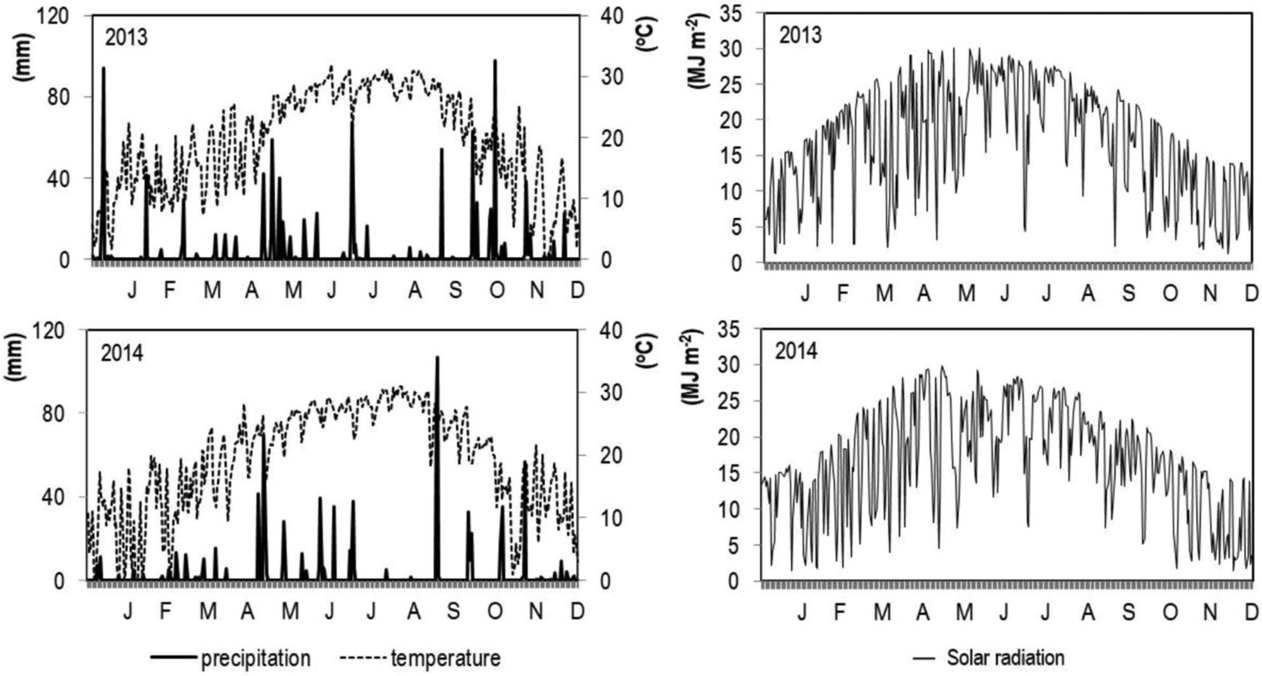

FIGURE 3 Daily mean air temperature, total rainfall, and solar radiation at Temple, TX in 2013 and 2014

LAI (DMLA), and then altering the LADC parameter values until an acceptable goodness-of-fit match was achieved. We used the measured optimum N and P concentrations in the tissue at early in the season (BN1 & BP1), mid-season (BN2 & BP2) and at maturity (BN3 & BP3) to simulate plant N and P nutrient uptake. We tested the accuracy of the developed plant parameters to predict vetivergrass biomass yields during the 2013 growing season.

Following successful ALMANAC parameterization and testing, we applied the model to assess vetivergrass' bioenergy feedstock production potential across Texas. Vetivergrass field management practices (Table 2), measured and derived plant parameters (Table 3) were combined with daily weather of representative weather stations for each ACZ (Figure 2) and SSURGO soil properties data of the dominant soil for each ACZ. Simulations were conducted for dryland and irrigated vetivergrass feedstock production systems, over a 41-yr time series (1970–2010), with the first year of the simulation being the grass establishment year. ALMANAC automatic N and P fertilizer and irrigation application options were applied to a level that did not impose any major nutrient and water stress constraints. We set the harvest efficiency to 90% of standing biomass.

3 | DATA ANALYSIS

The SAS (version 9.4) (SAS Institute, 2018) repeated measures ANOVA and standard errors for the mean at $p \leq .05$ were used to determine significant differences between measured variables: plant height, LAI, light extinction coefficient (k), RUE, plant tissue N and P concentrations, and biomass yields across seven biomass harvests. The SAS REG and CORR procedures was used to conduct regression analyses and to describe the relationship between measured variables. The RMSE was used to estimate the variation between simulated and field measured values. We used the coefficient of residual mass (CRM, Xevi, Gilley, & Feyen, 1996) to measure the tendency of the model to overestimate or underestimate the measured values. A negative CRM indicates a tendency of the model to overestimate, while a positive value indicates underestimation of measured values.

4 | RESULTS AND DISCUSSION

4.1 | Study site weather

Daily mean air temperature, solar radiation, and total rainfall during the 2013 and 2014 growing seasons (April to September) are presented in Figure 3. In 2013, the daily mean air temperature was 25°C, total rainfall, 403 mm, solar radiation, 21 MJ m^{-2} d^{-1}, wind speed, 2.6 m s^{-1}, and relative humidity of 62%. Except for the lower total rainfall (371 mm) in 2014, weather for 2014 during the study period was similar to 2013, and within the range of normal conditions for Temple, TX. The lower rainfall and distribution pattern in 2014 resulted in some water stress which impacted overall plant growth,

TABLE 2 Field management practices for vetivergrass grown at Temple, TX, 2012–2014. ALMANAC automatic N and P fertilizer and irrigation application options were used in the simulations to assess vetivergrass' feedstock production potential under rainfed and irrigated conditions across Texas

Field operation	Date	Attribute, depth, or amount
Herbicide application (Roundup)	Pre-plant	3.5 L ha^{-1}
Plow	Pre-plant	200 mm
Tandem disk	Pre-plant	100 mm
Nitrogen fertilizer	Pre-plant	120 kg N ha^{-1}
Phosphorus fertilizer	Pre-plant	30 kg P ha^{-1}
Plant	April, 2012	3–5 slips/hole
Mowing	September, 2012	15 cm height
Hand weeding	When needed, 2013	
Harvesting (Baler)	September, 2013	
Hand weeding	When needed, 2014	
Harvesting (Baler)	September, 2014	90%

TABLE 3 Measured and derived key growth parameters for vetivergrass

ALMANAC symbol	Definition	Parameter value
WA	Radiation use efficiency (g MJ^{-1} m^{-2})[a]	2.9
TOP	Optimal temperature for plant growth (°C)	30
TBS	Minimum temperature for plant growth (°C)	8
DMLA	Maximum leaf area index (LAI)	13.3
DLAI	Fraction of season when LAI declines	0.65
RLAD	Leaf area decline rate	0.12
DLAP1	First point on optimal LAI curve	35.20
DLAP2	Second point on optimal LAI curve	60.95
k	Light extinction coefficient	0.22
HMX	Maximum plant height (m)	2.2
HI	Harvest index (biomass)	0.9
BN1[b]	Nitrogen content at early season	0.0166
BN2[b]	Nitrogen content at mid-season	0.0109
BN3[b]	Nitrogen content at maturity	0.0080
BP1[b]	Phosphorus content at early season	0.0014
BP2[b]	Phosphorus content at mid-season	0.0010
BP3[b]	Phosphorus content at maturity	0.0008

[a]Referred to in ALMANAC as the Biomass-energy ratio.
[b]Normal fractions of N and P in biomass.

as evidenced by the reduced plant height, LAI, and biomass production.

4.2 | Plant height and biomass accumulation

There were significant plant height differences ($p < .01$) between the 2013 and 2014 growing seasons (Figure 4). For both years, plant height increased linearly, respectively reaching maximum plant heights of 2.2 ± 0.1 m and 1.9 ± 0.0 m, 127 days after green-up (DAG). Thereafter, plant height declined due to senescence. As pointed out earlier, plant height in 2014 was partly affected by the lower rainfall. While the vetivergrass showed no noticeable nutrient deficiency symptoms, reduced plant growth in 2014 could also be attributed in part to a decline in soil fertility since no fertilizer was applied in 2013 and 2014. The rate of increase in plant height was also lower in 2014 (95 mm d^{-1}) compared to 2013 (111 mm d^{-1}). Despite the tall plant height, no lodging was observed. Vetivergrass stems and leaf bases are stiff and strong, while the massive fibrous and deep roots provide extra support to resist lodging. Vetivergrass plant height of up to 2 m and a root system that can reach depths down to 2–6 m have been reported by Greenfield (1990) and Vieretz et al. (2003).

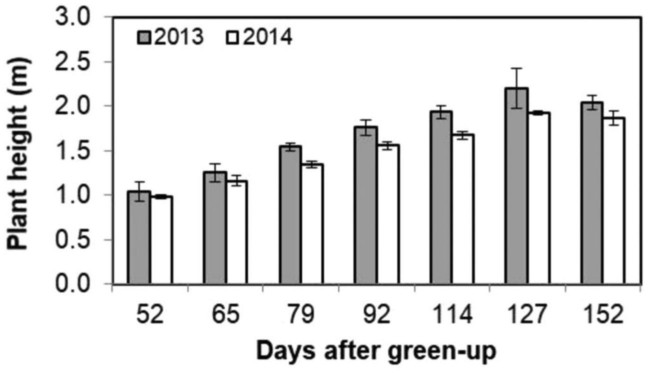

FIGURE 4 Vetivergrass plant height during the 2013 and 2014 growing seasons. Despite the tall plant height, no lodging was observed. Vertical bars are the SE values

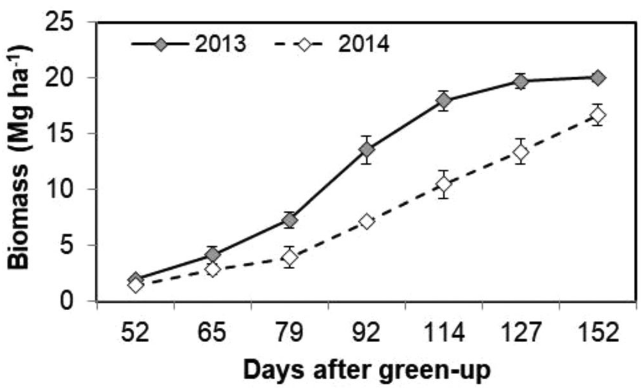

FIGURE 5 Biomass yields were noticeably lower in 2014 when compared to 2013 partly due to the drier conditions that affected plant growth. Vertical bars are the SE values

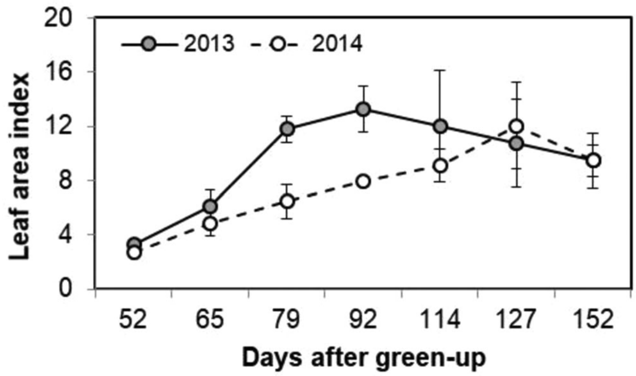

FIGURE 6 Vetivergrass leaf area index (LAI) development during the 2013 and 2014 growing seasons. Vertical bars are the SE values

Biomass yields were noticeably lower in 2014 when compared to 2013 (Figure 5). Again, these differences can be attributed partly to the 2013 and 2014 seasonal rainfall differences. In 2013, the vetivergrass tillered rapidly following green-up (Figure 1b), and like most C_4 plants was efficient in converting solar radiation to biomass. Biomass accumulation was rapid and followed the typical sigmoid growth curve pattern reaching a maximum yield of 20.1 ± 0.4 Mg ha^{-1}. In 2014, biomass accumulation was almost linear, reaching a maximum yield of 16.7 ± 1.0 Mg ha^{-1}. Biomass yields were lower in 2014 partly due to the lower rainfall during the vetivergrass rapid growth phase. However, besides rainfall, plant growth and biomass yield were reduced due to 'ratooning' effects. Several studies have reported reduced plant growth and biomass yield in ratooned bioenergy crops compared to the plant crop: sugarcane (Legendre & Burner, 1995), energy cane, biomass sorghum, switchgrass, giant miscanthus, big bluestem and giant reed, miscane (Burner, Hale, Carver, Porte, & Fritschi, 2015; Smith, Allen, & Barney, 2015), sweet sorghum (Duncan & Gardner, 1984), forage sorghum (Vinutha, Kumar, Blummel, & Rao, 2017). While ratooning has several advantages, more importantly, reduced costs of production through saving in land preparation and seed materials, the practice also has many disadvantages that include reduced plant growth and yield as a result of damage by pests and diseases, and a decline in soil fertility over time. Poor growth in ratooned crops is also due to less efficient water and nutrient uptake, due to suberized and aged root systems (Panwar, Verma, & Srivastava, 1989).

According to Vieretz et al. (2003), vetiver biomass yields usually range from 20 to 40 Mg ha^{-1} yr^{-1}. In many tropical countries, vetivergrass grows and survives on infertile soils without application of N and P fertilizers. Studies have shown that the vetivergrass establishes symbiotic associations with a wide range of soil microbes that include N fixing bacteria and P solubilizing mycorrhizal fungi (Siripin, 2000). Vetivergrass growth rates for the seven harvest intervals in 2013 and 2014 ranged from 3.8 ± 0.1 to 15.7 ± 0.1 and 2.7 ± 0.1 to 11.0 ± 0.1 g m^{-2} d^{-1}, respectively. Overall, there was a strong positive correlation (Pearson, r = 0.96) between plant height and biomass yield.

4.3 | Leaf area index and light interception

Leaf area index (LAI) development during the 2013 and 2014 growing seasons is shown in Figure 6. The LAI varied in response to the growing season, in particular rainfall (Figure 3). In 2013, higher rainfall during the green-up period triggered rapid tillering and leaf area development resulting in a maximum LAI of 13.3 ± 1.7, which occurred 92 days after observed green-up. In 2014, overall plant growth and leaf area development were slower earlier in the growing season, but LAI reached a peak of 12.0 ± 3.2, 127 days after observed green-up, spurred by the late growing season rainfall. Similar to plant height and biomass yield, the lower LAI in 2014 was most likely due to the combined effects of the lower precipitation and ratooning effects. As pointed out

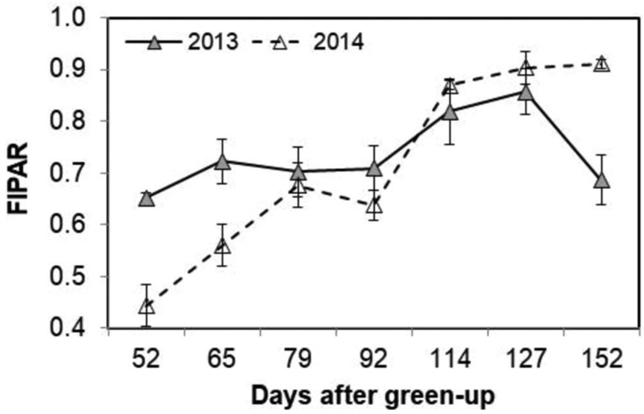

FIGURE 7 Water stress during the earlier part of the 2014 growing season resulted in reduced vetivergrass leaf area index (LAI) which was insufficient to intercept maximum photosynthetically active radiation (PAR) compared to the 2013 season. Vertical bars are the SE values

earlier, FIPAR is related to LAI through the Beer-Lambert equation (Monsi & Saeki, 1953) and normally increases over time (Figure 7) as LAI increases. Based on the data presented in Figure 7 we could not find a plausible explanation as to why some of the computed FIPAR readings for 2013 and 2014 (52, 65, and 152 DAG) differed so widely, even though their corresponding LAIs were not significantly different from each other. We can only speculate the possibility of errors in the PAR measurements, even though our ceptometer calibration readings were within the stipulated values. Light interception differences could also easily have been caused by leaf angle differences as affected by wind. Unlike most grasses which have a central stem and leaf structure, vetivergrass lacks a real stem and we observed that leaves were easily swayed from one direction to the other by even the smallest gusts of wind, as can be seen in Figure 1c.

Regrettably, no vetiver LAI data is readily available from the literature to compare with our observed values. Similar high LAI values have however been reported for other C_4 grasses such as switchgrass, 17.7 (Kiniry et al., 1999), napier grass, 15.4 (Kubota, Matsuda, Agata, & Nada, 1994), energy sorghum, 9.8 (Meki et al., 2017). There was a high positive correlation between LAI and biomass yield (Pearson, r = 0.77). For most crops, plant growth and biomass accumulation depend on the amount of IPAR, which is largely determined by LAI and numerous other environmental factors (Biscoe & Gallagher, 1975; Evans, 1993; Ewert, 2004; Monteith, 1978).

The light extinction coefficient (*k*) in the Beer-Lambert equation can be used to describe light interception efficiency per unit LAI (Kiniry et al., 1999). The relationship between *k* and LAI is shown in Figure 8. The *k* values were small and generally showed a decreasing trend with increasing LAI. Mean estimates of *k* for 2013 and 2014, averaged across

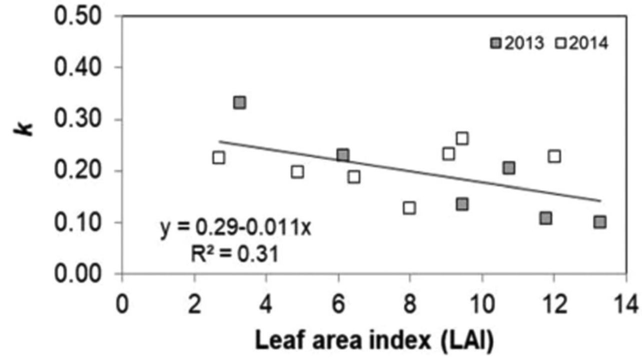

FIGURE 8 Relationship between leaf area index (LAI) and the light extinction coefficient (*k*) for vetivergrass for the Beer-Lambert equation over the 2013 and 2014 growing seasons. Mean *k* values were 0.22 ± 0.05 for 2013, and 0.21 ± 0.02 for 2014

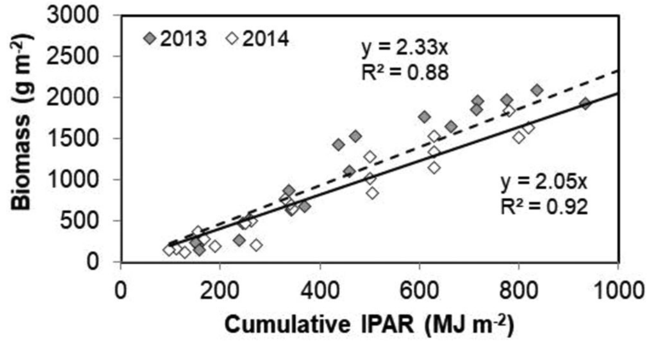

FIGURE 9 Vetivergrass radiation use efficiency calculated as the slope of the regression equations for dry biomass as a function of accumulated intercepted photosynthetically active radiation (IPAR)

the entire season, were 0.22 ± 0.05 and 0.21 ± 0.02. The stiff vetivergrass leafy stems impose an erectophile canopy structure for the most part of the growing season, with leaves becoming longer and horizontal only late in the season (Figure 1c). Plants with an erectophile canopy structure have smaller k values and have been shown to allow more light penetration into the canopy resulting in more efficient conversion of IPAR into biomass (Rhodes, 1971; Sheehy & Cooper, 1973). While vetivergrass had a very high LAI, the decrease in *k* with increasing LAI arguably improved light-penetration into the canopy.

4.4 | Radiation use efficiency

Radiation use efficiency was computed using the biomass yield and cumulative IPAR method (Figure 9) and was calculated as the slope of the regression equations for dry biomass as a function of accumulated IPAR. The RUE values for 2013 and 2014 were 2.3 ± 0.1 and 2.1 ± 0.1 g MJ^{-1}, respectively. Radiation interception depends on incident

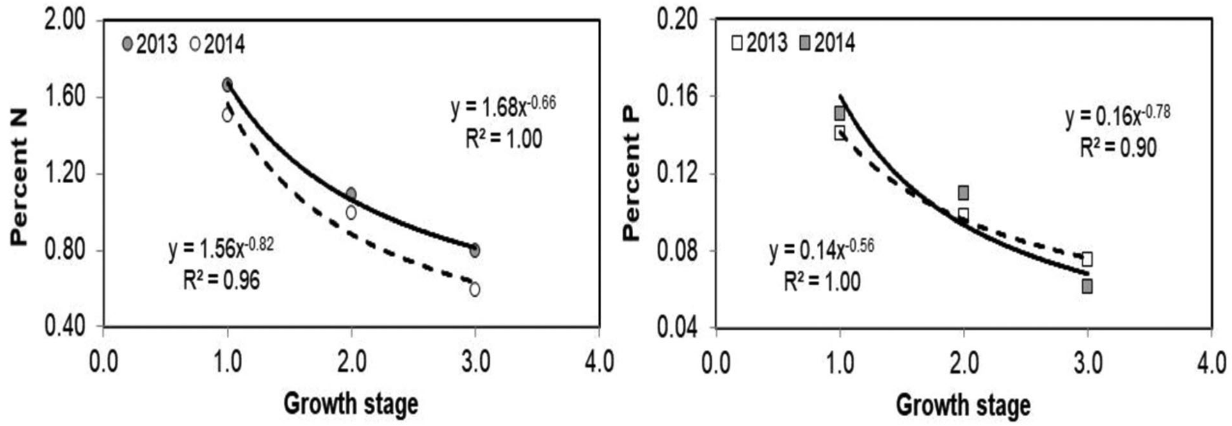

FIGURE 10 Vetivergrass plant tissue nitrogen (N) and phosphorus (P) concentrations at three growth stages: 1.0 early establishment; 2.0, mid-season; and 3.0, late-season (final harvest)

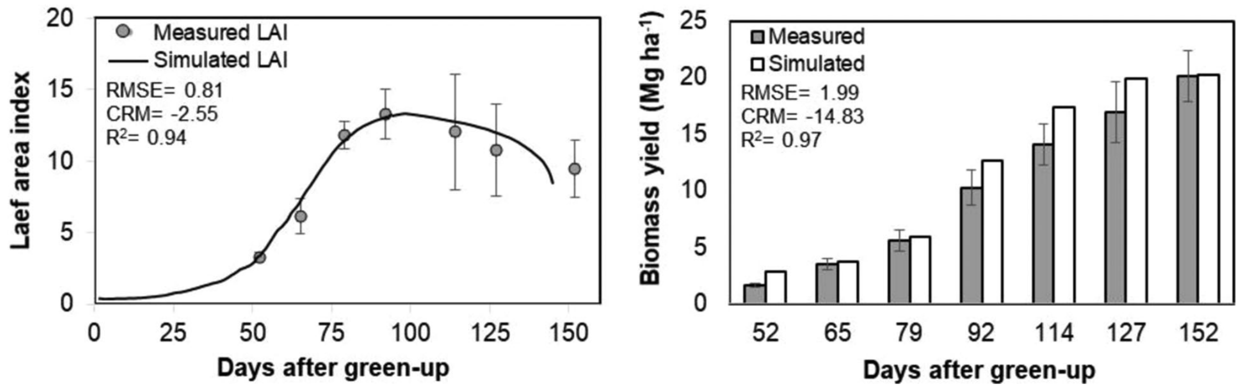

FIGURE 11 ALMANAC model simulation of vetivergrass (a) leaf area development, and (b) biomass yield at Temple, TX during the 2013 growing season. RMSE, root mean square error, CRM, coefficient of residual mass. Vertical bars are the SE values for the measured LAI values

radiation, LAI and *k* accounting for canopy architecture (Bonhomme, 2000; Kiniry et al., 1989; Lizaso, Batchelor, Westgate, & Echarte, 2003; Sadras, Villlobos, & Fereres, 2016). Differences in RUE in 2013 and 2014 can be attributed to differences in biomass accumulation which varied primarily due to differences in LAI and hence IPAR. Our estimated vetivergrass RUE values compare favorably to those of Vieretz et al. (2003) that were estimated at two sites in Australia: 1.8 and 2.1 g MJ^{-1}. Differences in reported estimates of RUE can be caused by a number of factors as discussed in Lindquist, Arkebauer, Walters, Cassman, and Dobermann (2005). According to Sinclair and Muchow (1999), experimental conditions and assumptions can result in a wide range of RUEs for the same crop.

4.5 | Plant tissue nitrogen and phosphorus concentration

Vetivergrass N uptake was lower throughout the drier 2014 season, while P uptake was lower during the first part of the season but recovered during the latter wetter part of the season. For both seasons, N and P concentrations decreased non-linearly as the season progressed (Figure 10). Averaged over years and across growth stages, N and P concentrations ranged from 0.59–1.66% and 0.06–0.15%, respectively. In pot trials, Wagner, Truong, and Vieritz (2003) reported minimum and maximum N and P concentrations required for vetiver growth of 0.2–2.5% and 0.07–0.16%, respectively. Under non-limiting soil moisture conditions, N and P play a critical role in determining plant growth and productivity parameters that include plant height, LAI, RUE and plant growth rate. Correct values for optimum N and P plant tissue concentrations are crucial for accurate simulation of plant uptake and nutrient balance (Kiniry et al., 2007).

4.6 | Derived plant growth parameters

The most critical plant parameters for simulating vetivergrass growth and biomass yield in ALMANAC are presented in Table 3. In ALMANAC, plant growth is simulated as

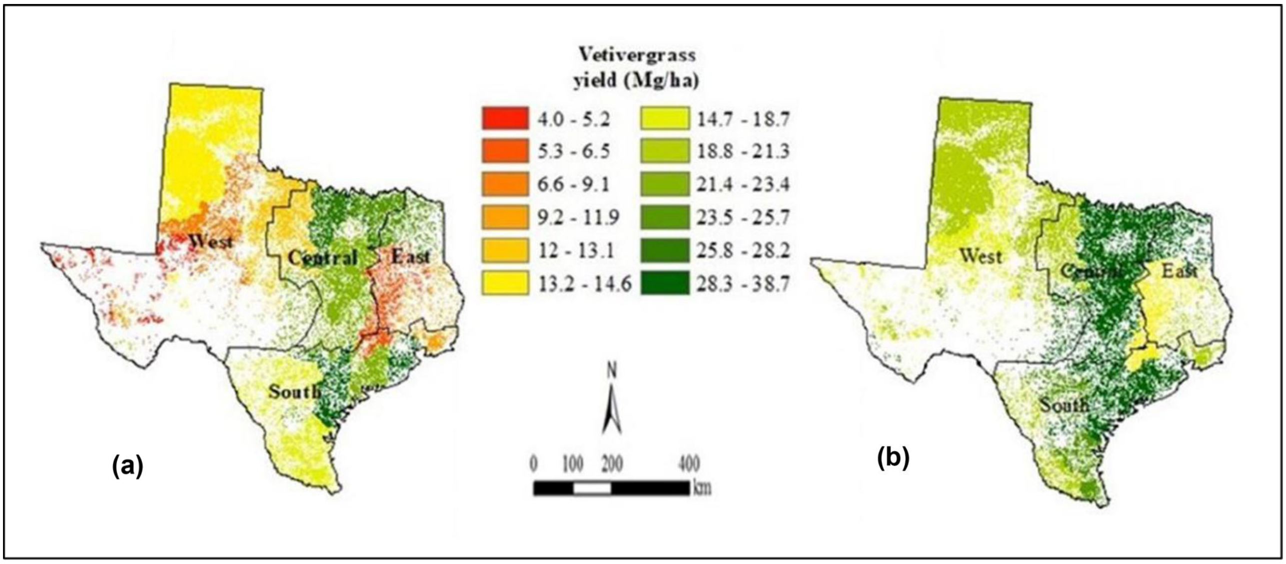

FIGURE 12 Twenty-year simulated average vetivergrass biomass yield under (a) dryland and (b) irrigated conditions across TX. Colored portions of the map also show where the potential target areas for vetivergrass feedstock production are distributed but does not imply that all the areas will be planted

TABLE 4 Dryland Production: Agroclimatic zones (ACZs), Texas region, soil type, rainfall, irrigation, average temperature, average biomass yield, yield standard deviation (SD) and total biomass production. ACZ ID# apply to Figure 2d in this study only and should not be used for any other purposes. The yield average and SD are based on 20-yr simulation data of continuous vetivergrass

ACZ ID#	Texas region	Area (ha)	Soil type (texture)	Rainfall (mm yr^{-1})	Avg. temp. (°C)	Avg. Yield (Mg ha^{-1})	Yield SD (Mg ha^{-1})	Total production (1000 Mg)
1	East	242,572	Loam	1,345	12	23.5	2.7	5,700
2	East	1,638,357	Sandy loam	1,172	18	22.6	2.8	37,027
3	East	827,373	Sandy loam	1,262	20	28.0	3.5	23,166
4	East	1,691,463	Loamy sand	1,126	20	22.4	3.3	37,889
5	South	1,030,056	Clay	1,117	21	25.7	4.5	26,472
6	South	1,064,024	Loam	871	21	21.3	4.0	22,664
7	Central	3,338,147	Clay loam	959	19	18.8	3.7	62,757
8	Central	1,623,564	Sandy loam	880	18	16.5	3.3	26,789
9	West	438,944	Clay	770	19	17.1	3.2	7,506
10	South	112,703	Sandy clay loam	1,230	21	24.2	4.4	2,727
11	South	2,036,215	Loam	657	22	14.8	3.5	30,136
12	South	1,081,418	Clay	498	22	13.2	3.9	14,275
13	West	3,140,454	Silty clay loam	655	17	14.4	2.7	45,223
14	West	2,217,504	Loam	517	17	11.0	2.7	24,393
15	West	21,117	Loam	562	20	11.9	4.1	251
16	West	74,510	Loam	379	19	6.6	3.4	492
17	West	804,519	Loam	316	17	5.2	3.0	4,183
18	West	144,146	Loam	446	16	9.3	3.3	1,341
19	West	28,250	Loam	294	21	5.9	2.4	167
20	West	6,963,318	Clay loam	516	15	10.9	2.2	75,900
21	South	363,762	Clay	1,354	21	31.4	4.0	11,422

TABLE 5 Irrigated Production: Agroclimatic zones (ACZs), Texas region, soil type, rainfall, irrigation, average temperature, average biomass yield, yield standard deviation (SD) and total biomass production. ACZ ID# apply to Figure 2d in this study only and should not be used for any other purposes. The yield average and SD are based on 20-yr simulation data of continuous vetivergrass

ACZ ID#	Texas region	Area (ha)	Soil type (texture)	Rainfall (mm yr^{-1})	Irrigation (mm)	Avg. temp. (°C)	Avg. yield (Mg ha^{-1})	Yield SD (Mg ha^{-1})	Total production (1000 Mg)
1	East	242,572	Loam	1,345	506	18	32.8	2.8	7,956
2	East	1,638,357	Sandy loam	1,172	572	18	32.1	2.9	52,591
3	East	827,373	Sandy loam	1,262	435	20	36.4	3.6	30,116
4	East	1,691,463	Loamy sand	1,126	461	20	29.7	3.3	50,236
5	South	1,030,056	Clay	1,117	491	21	32.1	5.0	33,065
6	South	1,064,024	Loam	871	495	21	27.7	4.5	29,473
7	Central	3,338,147	Clay loam	959	570	19	26.7	3.8	89,129
8	Central	1,623,564	Sandy loam	880	578	18	24.5	3.6	39,777
9	West	438,944	Clay	770	592	19	24.9	3.6	10,930
10	South	112,703	Sandy clay loam	1,230	504	21	30.2	4.5	3,404
11	South	2,036,215	Loam	657	484	22	19.6	4.2	39,910
12	South	1,081,418	Clay	498	593	22	19.1	4.8	20,655
13	West	3,140,454	Silty clay loam	655	555	17	23.4	3.1	73,487
14	West	2,217,504	Loam	517	533	17	20.6	2.8	45,681
15	West	21,117	Loam	562	518	20	19.4	4.3	410
16	West	74,510	Loam	379	554	19	15.7	3.6	1,170
17	West	804,519	Loam	316	572	17	15.8	3.5	12,711
18	West	144,146	Loam	446	525	16	20.5	4.0	2,955
19	West	28,250	Loam	294	517	21	13.6	3.0	384
20	West	6,963,318	Clay loam	516	593	15	21.6	3.0	150,408
21	South	363,762	Clay	1,354	476	21	38.7	4.3	14,078

a function of LAI and intercepted solar radiation, while biomass accumulation is simulated with a plant species-specific RUE (Kiniry et al., 1992). ALMANAC computes RUE based on total plant biomass that includes root biomass. The fraction of total biomass partitioned to the root system of most crops normally decreases from 0.30 to 0.50 in the seedling to 0.05 to 0.20 at maturity (Jones, 1985). The model simulates this partitioning by decreasing the fraction linearly from emergence to maturity. We applied the maximum root biomass fraction at maturity of 0.20 to our measured aboveground biomass which resulted in a RUE of 2.9 g MJ^{-1} m^{-2}. LAI development is simulated based on DMLA and LADC parameters (DLAP1, DLAP2, DLAI, and RLAD) that describe how LAI develops during the season. Optimum N and P plant tissue concentrations (BN1-3 and BP1-3) are used in simulating N and plant uptake and nutrient balance.

4.7 | ALMANAC parameterization and testing

ALMANAC simulations of vetivergrass leaf area development and biomass yield are presented in Figure 11. ALMANAC adequately predicted the 2013 vetivergrass leaf area development and biomass yields. The average of simulated LAI values (9.78) was close to the average of measured values (9.54) (RMSE, 0.81; CRM, −2.55; R^2, 0.94). Biomass yields were predicted with a RMSE of 1.99 kg ha^{-1} and a CRM of −14.83. ALMANAC overestimated both the LAI and biomass yields, especially after the fourth biomass sampling harvest (i.e., 92 DAG). The overestimation could also be the result of errors in the sampled measurements as indicated by the high standard errors for measurements gathered after the fourth harvest. As pointed out earlier, ALMANAC simulates plant growth as a function of LAI and intercepted solar radiation, while biomass accumulation is simulated with a plant species-specific RUE (Kiniry et al., 2007). Hence, good calibration of the LADC is crucial for accurate simulation of plant growth and biomass accumulation in ALMANAC.

4.8 | Simulation of vetivergrass feedstock production potential

4.8.1 | Agroclimatic zones

The rainfall and temperature gradients across Texas are respectively illustrated in Figure 2b and 2c, while the ACZs

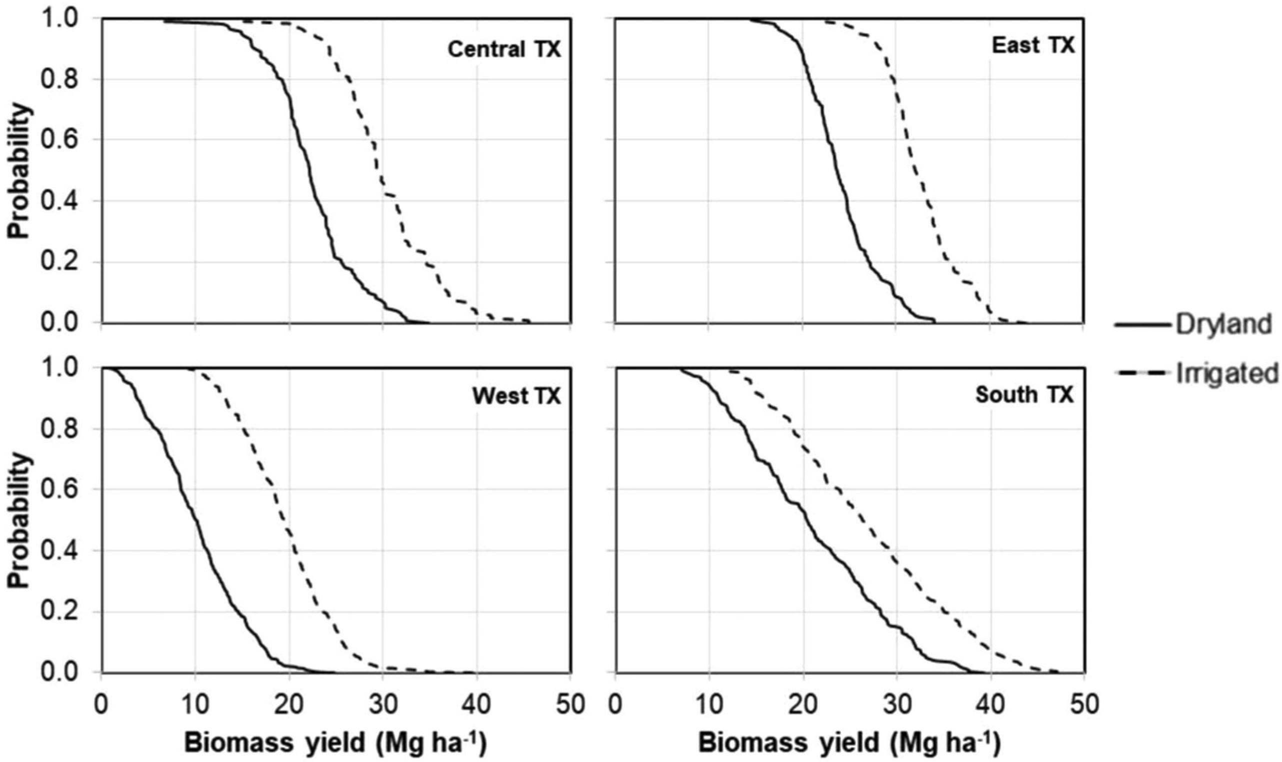

FIGURE 13 Cumulative probability of vetivergrass biomass yields across central, east, west and south TX under dryland and irrigated conditions over a 41-yr simulation timescale (1970–2010)

are shown in Figure 2d. Average annual rainfall across the ACZs during the 20-yr simulation period varies from a minimum of 294 mm to a maximum of 1354 mm. The rainfall shows a strong east to west gradient (Figure 2b), with some areas in east Texas receiving almost five times higher rainfall than areas in west Texas. Annual average temperatures vary between 12–22°C and follow a north-south gradient (Figure 2c). The north to south temperature gradient impacts biomass yields through high and low temperature stresses and its effects on the length of the growing season.

4.8.2 | Biomass yield

Vetivergrass biomass yields showed the expected east to west gradient for both dryland and irrigated production, with the highest yields broadly in the high rainfall Central-East-South Gulf Coast Prairie area (Figure 12). Irrigation increased biomass yields by on average 48%. Tables 4 and 5 summarize the biomass yields by ACZ identification number, Texas region and soil type. Dryland and irrigated biomass yields across the ACZs ranged from 5.2 to 31.4 (avg. 16.9) Mg ha^{-1} and 13.6 to 38.7 (avg. 25.0) Mg ha^{-1}, respectively. The standard deviations were respectively 3.4 and 3.7 Mg ha^{-1}. At Temple, TX, simulated dryland and irrigated yields in 2013 were 20.3 and 39.7 Mg ha^{-1}, respectively. There was high interannual variation in biomass yields for both dryland and irrigated conditions as indicated by the high CV percent values of 25 and 17%, respectively. As expected, dryland and irrigated biomass yields were respectively highly and positively correlated to the growing season rainfall (Pearson, r = 0.97, and R^2 = 0.93 at $p \le .05$) and total water inputs (rainfall plus irrigation) (Pearson, r = 0.92, and R^2 = 0.86 at $p \le .05$). Vetivergrass biomass yields up to two times greater than our yields have been reported in the tropics and subtropics (Bouchard, 2005; Pinners, 2014; Zarotti, 2002). Understandably, biomass yields vary depending on site-specific factors that include climate, soils, management, cultivar and years of crop establishment.

The ALMANAC auto-irrigation trigger on average applied 530 mm of water with slightly more in the low rainfall west Texas area (546 mm) and less in the east Texas area (467 mm). For the irrigated vetivergrass, about 21 mm of water was required to produce 1 Mg of harvested biomass. Likewise, the auto-N and P fertilizer triggers on average applied 153 kg N ha^{-1} and 57 kg P ha^{-1} in dryland areas, and 202 kg N ha^{-1} and 79 kg P ha^{-1} in irrigated areas. Nutrient uptake was higher under irrigated vetivergrass compared to dryland: 114 kg N ha^{-1} and 93 kg P ha^{-1}, and 83 kg N ha^{-1} and 68 kg P ha^{-1}, respectively. On average, each Mg of biomass harvested removed approximately 5 kg N ha^{-1} and 4 kg P ha^{-1}.

The predicted total vetivergrass biomass production across all ACZs is about 460 and 709 million Mg for dryland and irrigated areas, respectively. However, the irrigated production is only indicative of overall production potential since only 25% (2.5 million hectares) of Texas's cropland is currently irrigated (TWDB, 2011) compared to the simulated area of 28.9 million hectares. Even for dryland production, the type and amount of land area converted to vetivergrass will be influenced by many factors including feedstock price. Under both dryland and irrigated production, it would be desirable to target environments that can consistently produce the minimum profitable harvestable yield. If for dryland conditions that average annual biomass yield is approximately 10 Mg ha^{-1} (9. 4 Mg ha^{-1}, Mclaughlin et al., 2002; 11.2 Mg ha^{-1}, US DOE, 2006), then west Texas, despite its large area, should be ruled out because of low yields (Figures 12 and 13). In west Texas, the probability of obtaining dryland biomass yields ≥10.0 Mg ha^{-1} is less than 0.50, while in central and east Texas, biomass yields are always >10.0 Mg ha^{-1} (Figure 13). In south Texas, the probability of obtaining a yield ≥10 Mg ha^{-1} is 0.90.

Although it is unlikely that vetivergrass will displace all the areas simulated in the ACZs, for analytical purposes, if dryland vetivergrass production was dedicated to ACZs with a potential average annual biomass yield ≥10 Mg ha^{-1} (Table 4), and assuming a conversion efficiency of 330 liters of cellulosic ethanol per megagram of dry biomass (NREL, 2011), then Texas could produce approximately 150 billion liters of ethanol per year, an amount almost three times higher than the current Texas motor gasoline consumption of 54.1 billion liters (US DOE, 2019).

5 | CONCLUSIONS

We conducted a field study to determine and evaluate plant growth parameter attributes for high biomass yield in vetivergrass. Overall, the high biomass yield can be attributed to the high LAI and high crop growth rate. Biomass yield was highly correlated to plant height and LAI. For most plants, plant growth and biomass accumulation are a function of the IPAR, which is largely determined by LAI and other factors that include N and P uptake. As previously pointed out, N and P play critical roles in determining plant growth and productivity parameters that include plant height, LAI, RUE and plant growth rate.

Both state-wide and local assessments of vetivergrass feedstock production potential and inter-annual yield variability can be obtained by appropriately using simulation models such as ALMANAC. The field experiment provided valuable plant coefficients that we used to develop an ALMANAC vetivergrass model to simulate vetivergrass bioenergy feedstock production potential across Texas. As expected, vetivergrass biomass yields followed the east to west rainfall gradient for both dryland and irrigated production, with the highest yields broadly in the high rainfall Central-East-South Gulf Coast Prairie area. There was high interannual variation in biomass yields for both dryland and irrigated conditions. These state-wide simulation model assessments complement field studies in a cost-effective way, and we hope will further allow bioenergy companies and investors to better estimate biofuel production potential for new crops such as vetivergrass.

Finally, for a vetivergrass cultivar to be widely accepted for use on the continental USA, it must be sterile and non-invasive. As discussed previously, the Sunshine cultivar has done well in Florida, Louisiana and south Texas without showing signs of invasiveness. In Hawaii, the cultivar has long been used in soil conservation programs. The grass can be eliminated easily either by mechanical uprooting or spraying with glyphosate herbicide.

ACKNOWLEDGMENTS

Preparation of this manuscript was supported by the USDA-ARS, Grassland, Soil and Water Research Laboratory, Temple, TX, through Specific Cooperative Agreement: 58-6206-1-053. We sincerely thank Rick Greeson and summer student interns for field work and technical assistance. USDA is an equal opportunity provider and employer. Source of photo in Figure 1d: The Vetiver Network International (https://www.vetiver.org/).

ORCID

Manyowa N. Meki
https://orcid.org/0000-0003-3941-8300

REFERENCES

Biscoe, P. V., & Gallagher, J. N. (1975). Weather, dry matter production and yield. In *Environmental effects on crop physiology*. Proc. Symp. held at Lon–Ashton Research Station, University of Bristol, Bristol, UK. 13–16 Apr. 1975. New York, NY: Academic Press.

Bonhomme, R. (2000). Beware of comparing RUE values calculated from PAR vs. solar radiation or absorbed vs. intercepted radiation. *Field Crops Research*, *68*, 247–252. https://doi.org/10.1016/S0378-4290(00)00120-9

Boucard, G. R. (2005). An alternative energy for the Dominican Republic. Texarome Inc. Retrieved from http://www.vetiver.org/DR-alternative%20energy.pdf (accessed 15 Mar. 2019).

Burner, M. B., Hale, A. L., Carver, P., Porte, D. H., & Fritschi, F. B. (2015). Biomass yield comparisons of giant miscanthus, giant reed, and miscane grown under irrigated and rainfed conditions. *Industrial Crops and Products*, *76*, 1025–1032. https://doi.org/10.1016/j.indcrop.2015.07.071

Council, National Research. (1993). *Vetiver grass: A thin green line against erosion*. Washington, DC: The National Academies Press. https://doi.org/10.17226/2077

Duncan, R. R., & Gardner, W. A. (1984). The influence of ratoon cropping on sweet sorghum yield, sugar production, and insect damage. *Canadian Journal of Plant Science*, *642*, 261–273.

EEE. (European Environmental Agency). (2007). Estimating the environmentally compatible bioenergy potential from agriculture. EEA Technical Report12. Copenhagen, Denmark: European Environmental Agency.

Evans, L. T. (1993). *Crop evolution, adaptation and yield*. Cambridge, UK: Cambridge Univ. Press.

Ewert, F. (2004). Modelling plant responses to elevated CO_2: How important is leaf area index? *Annals of Botany*, *93*, 619–627. https://doi.org/10.1093/aob/mch101

Greenfield, J. C. (1990). Vetiver grass. *The hedge against erosion* (3rd ed.). Washington, D.C.: The World Bank.

Grimshaw, D. (2004). The vetiver system – Land stabilization and energy production. Vetiver Highlights No. 2. Retrieved from http://www.vetiver.org (accessed 20 Apr. 2019).

Jones, C. A. (1985). *C-4 grasses and cereals*. New York: John Wiley & Sons.

Kiniry, J. R., Jones, C. A., O'Toole, J. C., Blanchet, R., Cabelguenne, M., & Spanel, D. A. (1989). Radiation use efficiency in biomass accumulation prior to grain filling for five grain crop species. *Field Crops Research*, *20*, 51–64. https://doi.org/10.1016/0378-4290(89)90023-3

Kiniry, R. J., Tischler, C. R., & Van Esbroeck, G. A. (1999). Radiation use efficiency and leaf CO_2 exchange for diverse C_4 grasses. *Biomass and Bioenergy*, *17*, 95–112. https://doi.org/10.1016/S0961-9534(99)00036-7

Kiniry, J. R., Williams, J. R., Gassman, P. W., & Debaeke, P. (1992). A general process-oriented model for two competing plant species. *Transactions of the ASABE*, *35*, 801–810. https://doi.org/10.13031/2013.28665

Kiniry, J. R., Burson, B. L., Evers, G. W., Williams, J. R., Sanchez, H., Wade, C., … Greenwade, J. (2007). Coastal bermudagrass, bahiagrass, and native range simulation at diverse sites in Texas. *Agronomy Journal*, *99*, 450–461. https://doi.org/10.2134/agronj2006.0119

Kubota, F., Matsuda, Y., Agata, W., & Nada, K. (1994). The relationship between canopy structure and high productivity in napiergrass (*Pennisetum purpureum*, Schumach). *Field Crops Research*, *38*, 105–110. https://doi.org/10.1016/0378-4290(94)90004-3

Lavania, U., & Lavania, S. (2009). Sequestration of atmospheric carbon into subsoil horizons through deep-rooted grasses - vetiver grass model *Current Science*, *97*(5), 618–619.

Legendre, B. L., & Burner, D. M. (1995). Biomass production of sugarcane cultivars and early-generation hybrids. *Biomass Bioenergy*, *8*(2), 55–61. https://doi.org/10.1016/0961-9534(95)00014-X

Lindquist, J. L., Arkebauer, T. J., Walters, D. T., Cassman, K. G., & Dobermann, A. (2005). Maize radiation use efficiency under optimal growth conditions. *Agronomy Journal*, *97*, 72–78. https://doi.org/10.2134/agronj2005.0072

Lizaso, J. I., Batchelor, W. D., Westgate, M. F., & Echarte, L. (2003). Enhancing the ability of CERES-Maize to compute light capture. *Agricultural Systems*, *76*, 293–311. https://doi.org/10.1016/S0308-521X(02)00003-3

Mclaughlin, S. B., De la Torre Ugarte, G. G., Garten, C. T., Lynd, L. R., Sanderson, M. A., Tolbert, V. R., & Wolf, D. D. (2002). High-value renewable energy from prairie grasses. *Environmental Science & Technology*, *36*, 2122–2129.

Meek, D. W., Hatfield, J. L., Howell, T. A., Idso, S. B., & Reginato, R. J. (1984). A generalized relationship between photosynthetically active radiation and solar radiation. *Agronomy Journal*, *76*, 939–945. https://doi.org/10.2134/agronj1984.00021962007600060018x

Meki, N. M., Ogoshi, R. M., Kiniry, J. R., Crow, S. E., Youkhana, A. H., Nakahata, M. H., & Littlejohn, K. (2017). Performance evaluation of biomass sorghum in Hawaii and Texas. *Industrial Crops and Products*, *103*, 257–266. https://doi.org/10.1016/j.indcrop.2017.04.014

Metzger, M. J., Bunce, R. G. H., Leemans, R., & Viner, D. (2008). Projected environmental shifts under climate change: European trends and regional impacts. *Environmental Conservation*, *35*, 64–75. https://doi.org/10.1017/S0376892908004529

Monsi, M., & Saeki, T. (1953). Uber den Lichtfaktor in den Pflanzengesellschaften und sein Bedeutung für die Stoffproduktion. *Journal of Japanese Botany*, *14*, 22–52.

Monteith, J. L. (1978). Reassessment of maximum growth rates for C_3 and C_4 Crops. *Experimental Agriculture*, *14*, 1–5. https://doi.org/10.1017/S0014479700008255

Monteith, J. L. (1965). Light distribution and photosynthesis in field crops. *Annals of Botany*, *29*, 17–37. https://doi.org/10.1093/oxfordjournals.aob.a083934

NREL (National Renewable Energy Laboratory). (2011). Process Design and Economics for Biochemical Conversion of Lignocellulosic Biomass to Ethanol. Dilute-Acid Pretreatment and Enzymatic Hydrolysis of Corn Stover. Technical Report NREL/TP-5100-47764, May 2011. U.S. Department of Energy, Office of Energy Efficiency & Renewable Energy. Contract No. DE-AC36-08GO28308.

Panwar, B. S., Verma, R. S., & Srivastava, S. N. L. (1989). Growth and development of ratoon crop vis-à-vis plant crop. *Cooperative Sugar*, *20*(6), 409–410.

Pinners, E. (2014). Vetiver system: Reversing degradation on- and off-farm, to keep soil carbon in place, build up root biomass, and turn degraded areas into biofuel sources. In J. G. Goreau, R. W. Larson, & J. Campe (Eds.), *Geotherapy: Innovative methods of soil fertility restoration, carbon sequestration, and reversing CO_2 increase* (pp. 301–323). Proc. 3rd Int. Conf. Vetiver and Exhibition, Guangzhou, China: CRC Press Taylor & Francis Group.

Quinn, D. L., Gordon, D. R., Glaser, A., et al. (2015). Bioenergy feedstocks at low risk for invasion in the USA: A "White List" approach. *BioEnergy Research*, *8*, 471–481. https://doi.org/10.1007/s12155-014-9503-z

Rhodes, I. (1971). The relationship between productivity and some components of canopy structure in ryegrass (*Lolium* spp.). *Journal of Agricultural Science*, *77*, 283–292. https://doi.org/10.1017/S0021859600024436

Sadras, V. O., Villlobos, F. J., & Fereres, E. (2016). Radiation interception, radiation use efficiency and crop productivity. In F. Villalobos & E. Fereres (Eds.), *Principles of agronomy for sustainable agriculture* (pp. 169–188). New York: Springer International Publishing.

SAS Institute. (2018). SAS system. Release 9.4. SAS Institute, Inc., Cary, NC.

Sheehy, J. E., & Cooper, J. P. (1973). Light interception, photosynthetic activity, and crop growth rate in canopies of six temperate forage grasses. *Journal of Applied Ecology*, *10*, 239–250. https://doi.org/10.2307/2404727

Smith, L. L., Allen, D. J., & Barney, J. N. (2015). Yield potential and stand establishment for 20 candidate bioenergy feedstocks. *Biomass Bioenergy*, *73*, 145–154. https://doi.org/10.1016/j.biombioe.2014.12.015

Sinclair, T. R., & Muchow, R. C. (1999). Radiation use efficiency. *Advances in Agronomy*, *65*, 215–265. https://doi.org/10.1016/S0065-2113(08)60914-1
Singh, M. (2011). A strategy for sustainable carbon sequestration using vetiver. Retrieved from www.cmmacs.ernet.in/cmmacs/Publications/proj_docs/PDCM1101.pdf (accessed 21 Oct. 2018).
Siripin, S. (2000). Microbiology associated with the vetiver plant. Proc. 2nd Int. Vetiver Conf. (ICV-2). Jan. 18–22, 2000, Thailand.
Taranet, P., Wattanaprapat, K., Meesing, I., & Nopmalai, P. (2011). Carbon sequestration and carbon dioxide emission in vetiver grass cultivation areas. In Vetiver and climate change (p. 8–9). The 5th Int. Vetiver Conf. Oct. 28–30. Lucknow, India. p. 8–9.
The World Bank. (1995). Vetiver grass for soil and water conservation, land rehabilitation, and embankment stabilization. *A Collection of Papers and Newsletters Compiled by the Vetiver Network*. Grimshaw, G.R., and L. Helfer (Eds.) World Bank Technical Paper Number 273. Washington, D.C.: The World Bank.
Truong, P., & Hengchaovanich, D. (1997). Application of the vetiver grass system in land stabilization, erosion and sediment control in civil construction. Proc. Southern Region Symp., Queensland Department of Main Roads, Queensland, Australia.
Truong, P. (2002). Vetiver grass technology. In M. Maffei (Ed.), Vetiveria. *The Genus* Vetiveria (pp. 114–132). London and New York: Taylor and Francis Publishers.
Texas Water Development Board (TWDB). (2011). TWDB Report 378 – Irrigation Metering and Water Use Estimates: A Comparative Analysis, 1999–2007. July 2011. Texas Water Development Board, Austin. http://www.twdb.texas.gov/
USDA NRCS. (2019a). Pacific Islands Area Plant Materials Program. 'Sunshine' Vetivergrass *Chrysopogon zizanioides* (L.) Roberty. Washington, D.C.: USDA. Retrieved from https://plants.usda.gov/plantguide/pdf/pg_chzi.pdf (accessed 28 July 2019).
USDA NRCS. (2019b). Description of STATSGO2 Database. Washington, D.C.: USDA NRCS. Retrieved from https://www.nrcs.usda.gov/wps/portal/nrcs/detail/soils/survey/geo/?cid=nrcs142p2_053629 (accessed 2 June 2018).
Soil Survey Staff. (2011). Spatial and tabular data of the Soil Survey of Texas. Washington, D.C.: USDA NRCS. Retrieved from http://soildatamartnrcs.usda.gov/ (accessed 9 Oct. 2018).
US DOE. (2006).Breaking the biological barriers to cellulosic ethanol: A joint research agenda. DOE/SC-0095. Washington, D.C.: US Department of Energy Office of Science and Office of Energy.
US DOE. (2019).Energy Information Administration, State Energy Data System (SEDS), Table F3: Motor Gasoline Consumption, Price, and Expenditure Estimates, 2017. Washington, D.C.: US Department of Energy Office of Science and Office of Energy. Retrieved from https://www.eia.gov/state/seds/ (accessed 14 Feb. 2019).
Veldkamp, J. F. (1999). A revision of *Chrysopogon* Trin. including *Vetiveria* Bory (Poaceae) in Thailand and Malesia with notes on some other species from Africa and Australia. *Austrobaileya 5*(3), 503–533.
Vieretz, A., Truong, P., Gardner, T., & Smeal, C. (2003). Modelling Monto vetiver growth and nutrient uptake for effluent irrigation schemes. In J. G. Goreau, R. W. Larson, & J. Campe (Eds.), *Geotherapy: Innovative methods of soil fertility restoration, carbon sequestration, and reversing CO_2 increase* (pp. 87–99). Proc. 3rd Int. Conf. Vetiver and Exhibition, Guangzhou, China: CRC Press Taylor & Francis Group.
Vinutha, K. S., Kumar, G. S. A., Blummel, M., & Rao, P. S. (2017). Evaluation of yield and forage quality in main and ratoon crops of different sorghum lines. *Tropical Grasslands*, *5*(1), 40–49. https://doi.org/10.17138/TGFT(5)40-49
Wagner, S., Truong, P., Vieritz, A. et al. (2003). Response of vetiver grass to extreme nitrogen and phosphorus supply. In J. G. Goreau, R. W. Larson, & J. Campe (Eds.), *Geotherapy: Innovative methods of soil fertility restoration, carbon sequestration, and reversing CO_2 increase*. Proc. 3rd Int. Conf. Vetiver and Exhibition, Guangzhou, China: CRC Press Taylor & Francis Group.
Xevi, E., Gilley, J., & Feyen, J. (1996). Comparative study of two crop yield simulation models. *Agricultural Water Management*, *30*, 155–173. https://doi.org/10.1016/0378-3774(95)01218-4
Zarotti, C. (2002). Collection, harvesting, processing, alternative uses and production of essential oil. In M. Maffei (Ed.), Vetiveria. *The Genus* Vetiveria (pp. 191). London and New York: Taylor and Francis Publishers.

SUPPORTING INFORMATION

Additional supporting information may be found online in the Supporting Information section at the end of the article.

How to cite this article: Meki MN, Kiniry JR, Worqlul AW, et al. Field and simulation-based assessment of vetivergrass bioenergy feedstock production potential in Texas. *Agronomy Journal*. 2020;112:2692–2707. https://doi.org/10.1002/agj2.20226